JOURNAL OF MATERIALS SCIENCE 26 (1991) 6300–6308

Interface reactions between titanium thin films and $(1\bar{1}2)$ sapphire substrates

J. H. SELVERIAN
GTE Laboratories, 40 Sylvan Road, Waltham, MA 02254 USA and Department of Materials Science and Engineering, Lehigh University, Bethlehem, PA 18015 USA

F. S. OHUCHI
E.I. du Pont de Nemours and Company, Central Research and Development Department, Experimental Station, Wilmington, DE 19880-0356 USA

M. BORTZ
Department of Applied Physics, Stanford University, Stanford, CA 93405 USA

M. R. NOTIS
Department of Materials Science and Engineering, Lehigh University, Bethlehem, PA 18015 USA

We have studied the reactivity of Ti with the R-plane $(1\bar{1}2)$ of sapphire from room temperature to 1250 °C by X-ray photoemission spectroscopy (XPS), transmission electron microscopy (TEM), X-ray diffraction (XRD), and Rutherford backscattering spectroscopy (RBS). The combination of these techniques allowed the interface reactions to be studied from the monolayer regime up to the bulk regime. XPS showed that at room temperature, monolayer coverages of Ti reduced the sapphire surface to form Ti–O and Ti–Al bonds. TEM, XRD, and RBS showed that annealing of room-temperature deposited Ti resulted in an interfacial region consisting of two layers, a $Ti_3Al[O]$ layer adjacent to the sapphire and a $Ti_{0.67}[O_{0.33}]$ layer at the free surface. The growth of the $Ti_3Al[O]$ layer had an activation energy of 103.4 ± 25 kJ deg-mole. The nature of the interfacial reaction between Ti and sapphire was similar for Ti coverages from the monolayer to the bulk regime.

1. Introduction

Many applications require joining metals to ceramics. Silicon semiconductor devices used in microelectronics are frequently mounted in alumina packages for protection from the environment. Connections from the chip to the outside world are made by depositing various metals on the alumina package [1]. In metal matrix composites the adhesion between the metal matrix and the ceramic reinforcing fibres is critical for a strong stable composite [2]. The physical quality and mechanical integrity of the matrix/fibre interface determines how effectively the loads are transferred from the matrix to the fibres. Titanium coatings are also used on Al_2O_3 ceramics to promote wetting in ceramic-to-metal brazed joints.

The reactions between metals and ceramics are important for the adhesion and long-term stability of these metal/ceramic systems. For this reason we chose to study the reactive Ti/sapphire system.

2. Background

2.1. Reactions between titanium and sapphire

Several previous studies of the Ti/sapphire system are in disagreement about the nature of the reaction at the Ti/sapphire interface. These studies are reviewed to highlight the discrepancies.

Chaug *et al.* [3] deposited Ti on to bulk crystals of the (0 0 1) surface of sapphire in a 10^{-7} Pa vacuum and studied the chemical reactivity with X-ray photoemission spectroscopy (XPS). Formation of a TiO_x $(1 < x < 1.5)$ compound was observed at a coverage of ~ 0.35 nm of Ti on sapphire. No change in the Al(2p) peak was observed indicating that no Al–O bonds were broken. However, evidence for local rearrangement of the bulk sapphire structure at the interface was seen. The Ti–O bonds that formed at the interface acted to "bridge" across the interface and join the bulk Ti and sapphire lattices.

Zhao *et al.* [4] considered reactions between 200 nm thick transition metal films with crystalline and amorphous Al_2O_3. Films of several metals were sputter deposited on the Al_2O_3 substrate which were then annealed at 800–900 °C for 2 hours in a vacuum of 3×10^{-7} Pa. Rutherford backscattering spectroscopy (RBS) and X-ray diffraction (XRD) studies suggested that an interlayer of TiAl and an outer layer of TiO formed. They calculated the heat of formation of the TiAl and TiO compounds. Their calculations showed that Ti may be able to reduce Al_2O_3 in the temperature range of 800–900 °C.

0022–2461/91 $03.00 + .12

Choi *et al.* [5] studied reactions between Ti and Ni with Al_2O_3 and Y_2O_3. Powders of Ti and Al_2O_3 were mixed (20 v/o Al_2O_3 + 80 v/o Ti), dry pressed, and sintered in argon for 5–20 hours at temperatures ranging from 650–1300 °C. XRD and electron microprobe analysis of the sintered composites revealed that after 5 hours at 650 °C, $Ti_3Al[O]$ and Ti[O] were formed and both phases had oxygen in solid solution. They proposed the following reaction

$$9Ti + Al_2O_3 = 3Ti[O] + 2Ti_3Al[O] \quad (1)$$

Lefakis *et al.* [6] studied reactions between 100 nm thick films of Al_2O_3 and monolayer coverages of Ti with Auger electron spectroscopy (AES) and ultraviolet photoelectron spectroscopy in a 10^{-8} Pa vacuum. The Al_2O_3 was thermally grown on metallic Al and was probably cubic γ-Al_2O_3 not hexagonal α-Al_2O_3 (sapphire). Ti reduced Al_2O_3 at room temperature to produce a 1 nm thick layer which was a mixture of TiO_2 and Al in accordance with the reaction proposed by Lofton and Swartz [7]

$$3Ti + 2Al_2O_3 = 4Al + 3TiO_2 \quad (2)$$

2.2. Kinetics of the reaction between titanium and sapphire

Chamberlain [8] studied 185 nm thick Ti films on sapphire substrates with AES in the temperature range of 566–484 °C. Fitting his data to Equation 3 below gave an activation energy of 170 kJ/deg-mole and a k_0 of 1.2×10^8 nm^2/s.

$$W^n = kt \quad (3)$$

$$k = k_0 \exp(-Q/RT) \quad (4)$$

Here W is the width of the layer, n is a growth exponent, t is the reaction time, k is the penetration constant, k_0 is a constant, and T is the reaction temperature in K [9, 10]. The slope of an Arrhenius plot of Equation 4 equals $-Q/R$, where Q is the activation energy and R is the gas constant. Tressler *et al.* [11] studied sapphire-reinforced Ti composites and found an activation energy of 215.6 kJ/deg-mole and a k_0 of 3×10^{13} nm^2/s. Both Chamberlain and Tressler found that the reaction between Ti and sapphire was diffusion controlled. However, both reported different activation energies for the diffusion process.

Several studies have dealt with the reactions between Ti and Al_2O_3, and different reactions and different reaction kinetics were reported. In the present study different experimental techniques are used to arrive at a self-consistent picture of the reactions and reaction kinetics between Ti and Al_2O_3.

3. Experimental procedure

Single crystals of $(1\,\bar{1}\,2)$ oriented sapphire were used in all of the investigations. The $(h\ k\ l)$ hexagonal index notation was used to describe all planes. XPS was preformed using monochromatized AlK_α X-rays (1.46 keV) and a hemispherical energy analyser with a resolution of 0.9 eV. The sapphire substrates were mounted on a heating stage in an ion-pumped ultra-high vacuum (UHV) chamber with base pressure of 10^{-8} Pa.

All samples were prepared in the analysis chamber to minimize surface contamination. The sapphire surface was cleaned by standard ion bombardment and heating techniques before Ti deposition. Carbon contamination was absent, as judged by XPS. Ti was deposited by resistively heating Ti ribbon. Temperatures from 25 °C to 1250 °C were studied and the sample temperature was measured with a thermocouple or an optical pyrometer. At temperatures greater than 500 °C the error was ±20 °C while at lower temperatures the error was ±75 °C.

Changes in the Al(2p), O(1s), and Ti(2p) core level positions and changes in the valence band were monitored as a function of temperature and Ti coverage. Absolute binding energies were not obtained because of sample charging, even though an electron flood gun was used to neutralize the charge build-up.

For XRD, RBS, and transmission electron microscopy (TEM), between 200–400 nm of Ti was RF radio frequency sputter deposited on sapphire substrates in a turbomolecular pumped vacuum chamber with a base pressure of 10^{-6} Pa. Titanium was sputtered from 99.7% pure sheet. Pre-deposition sputtering cleaned any absorbed molecules from the Ti target. The Al_2O_3 substrates were held at temperature: 525, 554, 562, 580, 630, and 663 ± 5 °C, during the entire 2 hour Ti deposition. The temperature of the samples was monitored with a thermocouple spot welded to tantalum foil clamping the sample to the heating furnace.

RBS was preformed using either 2.25 or 2.8 MeV $^4He^+$ ions. Spectra were converted into composition and distance according to the methods outlined by Chu *et al.* [12]. The width of the Ti and Al peaks were set equal to the composition limits of the Ti_3Al phase on the Ti–Al binary phase diagram, since access to computer routines for spectra deconvolution was not available.

Cross-section samples of the annealed Ti/sapphire samples were studied by TEM. A Philips 430 TEM with a windowless energy dispersive X-ray energy dispersive spectroscopy (XEDS). All of the reported chemical compositions were corrected for X-ray absorption. The foil thickness was determined by a convergent beam electron diffraction (CBED) technique [13].

4. Results and discussion

4.1. Reactions between titanium and sapphire

4.1.1. XPS investigation

The phrase "metallic aluminum" or "metallic titanium" is used to refer to metallic type of bonding and not pure, elemental Al or Ti. A series of experiments were carried out to determine the effect of temperature on the reaction between Ti and sapphire.

Fig. 1a and b show the Al(2p) peaks for increasing Ti coverage at 25 °C and 1000 °C, respectively. Low, medium, and high coverages correspond approximately to one, two, and four equivalent monolayers. At low Ti coverages, an additional peak developed on the

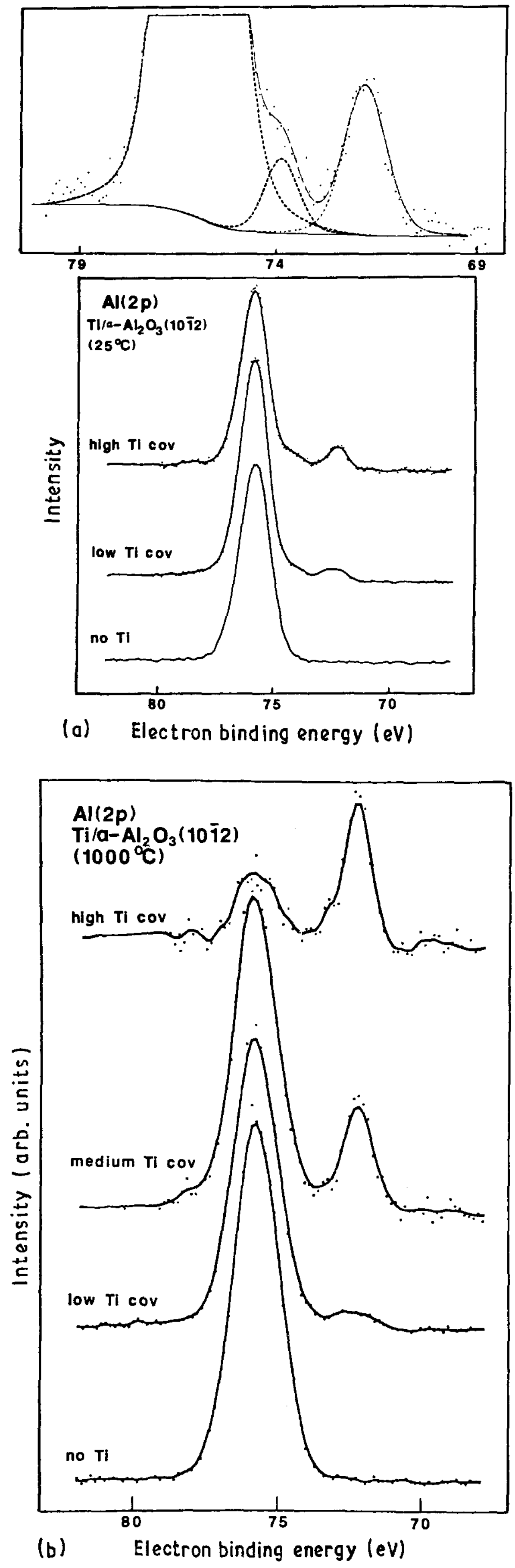

Figure 1 Al(2p) peaks as a function of Ti coverages at (a) 25 °C and (b) 1000 °C.

low binding energy side of the Al(2p) peak. This peak corresponds to metallic Al, indicating that Ti reduced the sapphire surface. At 25 °C, the metallic Al peak slowly grew with increasing coverage. However, at 1000 °C the metallic Al peak developed considerably, indicating that the majority of Al–O bonds in the surface region were reduced.

The process involved in the Ti-induced reduction of sapphire was further investigated by ramping the substrate temperature from 25 °C to 1250 °C, during which the changes observed in the Al(2p) were recorded, as shown in Fig. 2. Room-temperature deposition of Ti (four equivalent monolayers) on sapphire induced a small fraction of metallic Al to form. As the temperature was increased, the reduced species, Al^0, grew as a function of temperature, and correspondingly, the Al^{3+} peak decreased. Upon further heating of the substrate to temperatures higher than 1200 °C, the metallic Al^0 peak abruptly disappeared. A simultaneous mass spectrometer measurement showed the evolution of a peak at $m/e = 13$ near 1200 °C, indicating Al sublimation from the system. No Ti mass signal was detected.

Reduction of sapphire to Al by Ti followed by Al desorption suggests that an intermetallic Al–Ti alloy formed. If the Al existed as pure Al it should have evaporated at a temperature well below 1200 °C (Fig. 3). The instability of the Al–Ti intermetallic species at high temperature may arise from the nature of the extremely thin film and the combination of high vacuum and high temperature. The surface, after losing the metallic Al species at high temperatures, consisted of Al^{3+} and Ti^{2+}, indicating Ti–O–Al bond formation.

The valence band region, as a function of temperature, is shown in Fig. 4. As the temperature increased, the intensity of the Ti(3d) orbital near the Fermi level decreased, indicating that the electron population of the Ti(3d) orbital decreased with temperature. A new orbital appeared at 8.0 eV and grew with temperature. This suggests that charge transfer between the Ti(3d) and O(2p) orbitals occurred.

After ramping the sample to 1250 °C it was held at temperature for 2 hours. The Ti(2p) region (Fig. 5), shows that Ti existed in two different chemical states corresponding to Ti(2p$_{3/2}$) peaks at 453.2 eV (peak A)

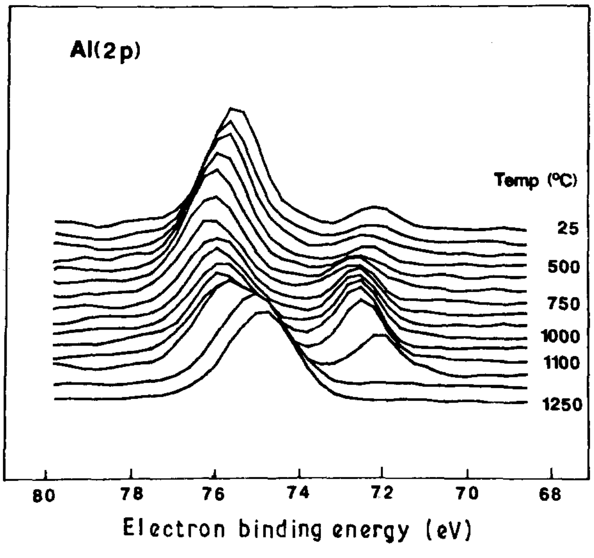

Figure 2 Al(2p) peak as a function of temperature, from 25 °C to 1250 °C. Near 1000 °C the metallic Al peak abruptly disappeared.

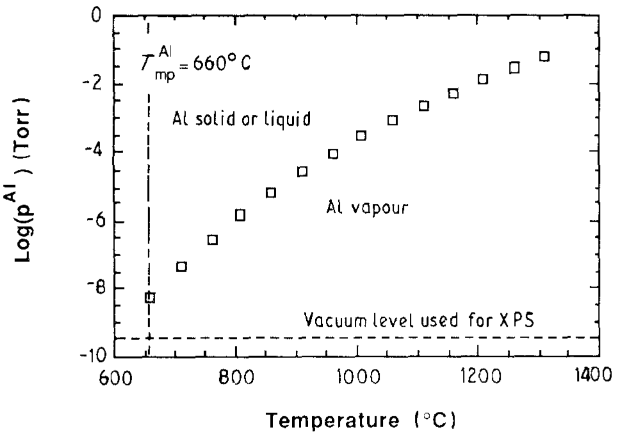

Figure 3 Plot of the log of the equilibrium pressure of Al as a function of temperature [21]. At the pressure levels used in XPS any pure Al metal would evaporate at temperatures above the melting point of Al, i.e., 660 °C.

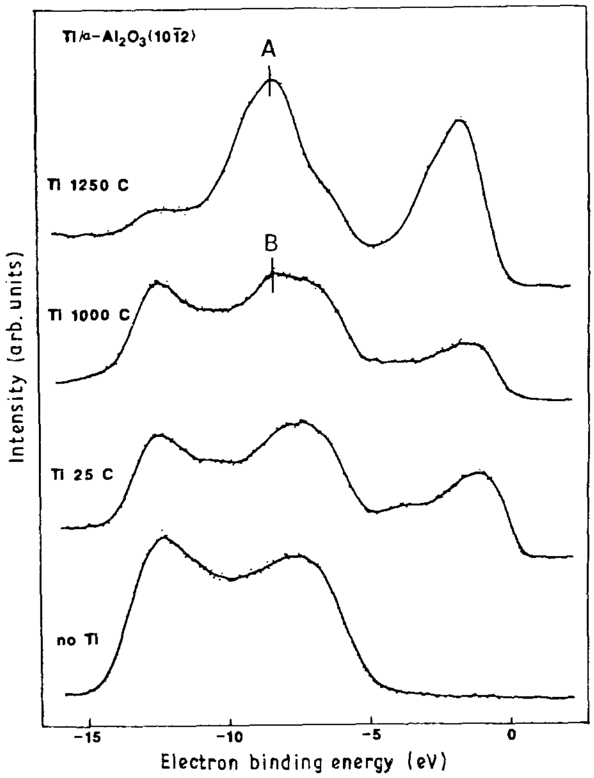

Figure 4 The valence band region from room temperature to 1250 °C.

and 455.6 eV (peak B). The energy difference between these two Ti($2p_{3/2}$) peaks is 2.4 eV. These peaks were fitted such that the peak area ratios A/C and B/D were 2/1, the natural intensity ratio for Ti($2p_{3/2}$)/Ti($2p_{1/2}$). A shift of the Ti($2p_{3/2}$) peak by 2.4 eV with respect to metallic Ti corresponds to Ti in a 2+ oxidation state [14]. No evidence was seen for Ti^{4+} or Ti^{3+}. The absence of the Ti^{3+} oxidation state indicates that Ti did not substitute for Al in the Al_2O_3 lattice, within the sensitivity of XPS.

The bonding across the Ti/sapphire interface is shown schematically in Fig. 6. The Ti near the interface formed bonds predominantly with oxygen. The Ti also bonded with the Al in the top layer of the sapphire, forming a mixed bonding involving Al, O, and Ti. As time progressed the interface mixed; metallic Ti–Al bonds formed as the sapphire decomposed into Al and O; and O diffused into the Ti film.

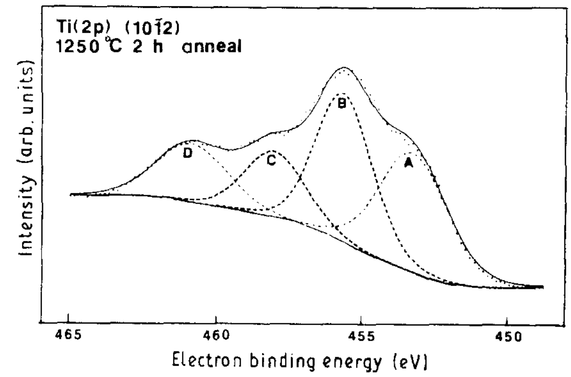

Figure 5 Ti(2p) peaks after a 2 hour anneal at 1250 °C. The Ti(2p) peak-split into 2 pairs of peaks (A–C) and (B–D). These peaks were fitted such that the peak area ratios A/C and B/D were 2/1, the natural intensity ratio for Ti($2p_{3/2}$)/Ti($2p_{1/2}$).

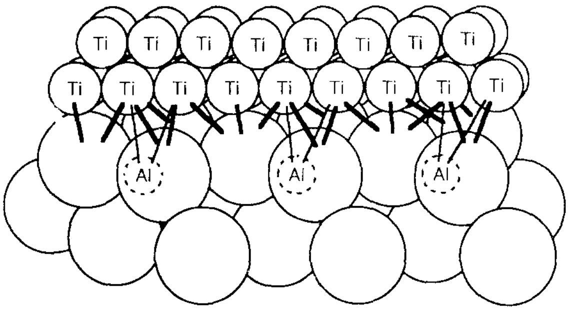

Figure 6 A schematic of the bonding between Ti and the (1 Ī 2) plane of sapphire. The Ti near the interface of sapphire bonds predominantly with oxygen, indicated by large circles. The Ti also bonds with the Al in the top layer of the sapphire, forming a mixed bonding involving Al, O, and Ti.

4.1.2. XRD, RBS, and TEM investigations

A series of XRD spectra, RBS spectra, and TEM micrographs were obtained after heat treating 200–400 nm thick Ti films on sapphire substrates at 25, 525, 554, 562, 580, 630, 663, and 825 °C for 2 hours.

Selected TEM micrographs are shown in Figs 7–10. The grain size of the Ti film was 30 nm for films deposited at 25 °C (Fig. 7) and 150 nm for films deposited at the elevated temperatures (Figs 8–10). All of the CBED patterns were indexed as disordered Ti_3Al. RBS indicated that all of the films contained 20–35 at. pct. oxygen and consisted of two layers, $Ti_3Al[O]$ adjacent to the sapphire, and $Ti_{0.67}[O_{0.33}]$ at the free surface. $Ti_3Al[O]$ refers to Ti_3Al with oxygen in solid solution and $Ti_{0.67}[O_{0.33}]$ refers to Ti with oxygen in solid solution. A typical RBS spectrum is shown in Fig. 11. The composition of the $Ti_3Al[O]$ layer, determined by TEM/AEM, was approximately 60 Ti, 23 Al, 22 O (at. pct.). Table I lists the thickness and composition of the $Ti_{0.67}[O_{0.33}]$ and $Ti_3Al[O]$ layers found in each sample, as determined by RBS and TEM/AEM.

Fig. 10 shows two different regions of the same sample annealed at 663 °C for 2 hours. These two micrographs show different microstructures indicating

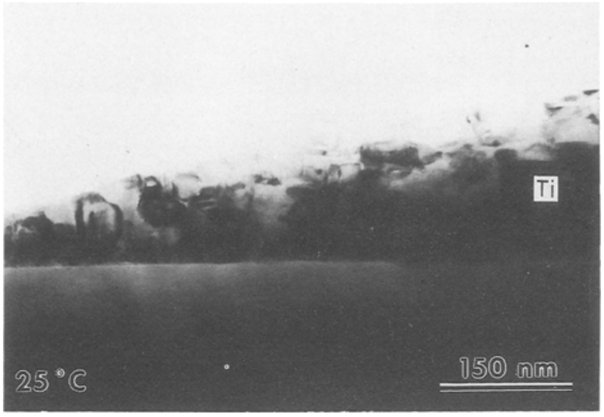

Figure 7 TEM image of sample deposited at 25 °C.

that there was a temperature gradient across the sample. The wavy interface structure in Fig. 10b suggests that the diffusional fluxes are unstable, leading to regions of supersaturation. This is typically referred to as interface breakdown. Interface breakdown can only occur in ternary or higher order systems [15].

The thickness of the $Ti_3Al[O]$ layer measured by TEM and RBS agreed well with one another. A large part of the error in the layer thicknesses was due to the existence of a temperature gradient across the samples. In the TEM/AEM measurements the error was due to only a very small region of the interface being actually observed. In the RBS measurements the error was related to difficulties in deconvoluting the spectra.

All of the Ti films exhibited a strong (0 0 2) texture, except for the film deposited at 554 °C which showed no obvious texture. The $Ti_3Al[O]$ layer had a range of textures suggesting that no strong texture existed for the $Ti_3Al[O]$ layer (Table II). Fig. 12 shows a CBED pattern encompassing several grains in the Ti film from the 25 °C sample. This pattern shows that there was no preferred orientation of the Ti grains with respect to the sapphire. Comparing this CBED pattern with the XRD results indicates that the film was deposited with the *c*-axis of Ti perpendicular to the sapphire substrate, but that all other degrees of freedom for crystal alignment were undetermined.

An additional sample to those mentioned above was made in the UHV chamber. This sample had 200 nm of Ti evaporated at room temperature and was annealed for 2 hours at 825 °C, all in a vacuum of 10^{-8} Pa [16]. The entire Ti film in this sample had transformed into a new, single-phase product. This phase was identified by TEM/AEM and CBED as ordered Ti_3Al with a composition of 64 ± 4 Ti, 24 ± 5 Al and 12 ± 6 O (at. pct.). The atomic ratio Al/O in the Ti_3Al layer should be 2/3, the same as in sapphire. However, the measured atomic ratio Al/O was 2/1 (allowing for worst-case errors it ranged from 4.8 to 1). This implied that oxygen diffused out of the Ti_3Al during annealing in the UHV chamber and indicates that the vacuum level has a significant effect on the final oxygen composition of the reaction layer.

4.2. Thermodynamics of the reaction between titanium and sapphire

The information obtained in the previous sections allows for a thermodynamic treatment of the reaction

TABLE I Layer thickness and compositions determined by TEM and RBS

Heat treatment temperature (± 5 °C)	Thickness of Ti_3Al layer TEM (nm, ± 20%)	RBS	Composition of layer by RBS (Ti, Al, O at. pct.)	
				Ti_3Al
25	0	–	–	–
525	65	59	82,0,18	57,21,22
554	82	100	68,0,32	60,20,20
562	72	79	75,0,25	58,20,22
580	117	100	66,0,34	56,23,21
630	120	138	76,0,24	62,24,14
663	220	217	75,0,25	60,25,15

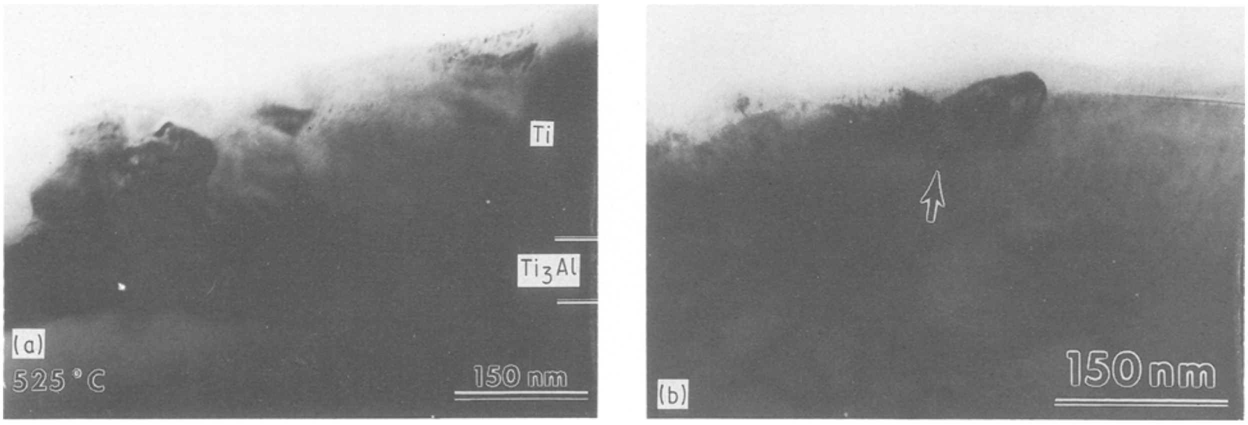

Figure 8 TEM images of samples deposited and annealed for 2 hours at 525 °C. The arrow in (b) indicates the Ti_3Al phase. The Ti_3Al is not continuous in this region.

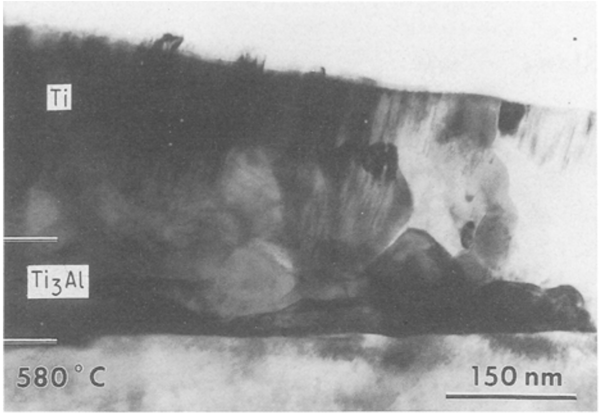

Figure 9 TEM image of a sample deposited and annealed for 2 hours at 580 °C.

between Ti and sapphire. The reaction products have been identified as $Ti_{0.67}[O_{0.33}]$ and $Ti_3Al[O]$ and the reaction between Ti and sapphire can be written as the sum of Equations 5–8

$$Al_2O_3 = 2Al + \tfrac{3}{2}O_2 \tag{5}$$

$$2\{3Ti + Al = Ti_3Al\} \tag{6}$$

$$3\{0.67Ti + 0.165O_2 = Ti_{0.67}[O_{0.33}]\} \tag{7}$$

$$2\{Ti_3Al + 1/2O_2 = Ti_3Al[O]\} \tag{8}$$

$$8Ti + Al_2O_3 = 3Ti_{0.67}[O_{0.33}] + 2Ti_3Al[O] \tag{9}$$

$$\text{Free Energy} = -431\,800 + 3.98T\mathrm{Ln}(T) - 87.64T \tag{10}$$

The net reaction, Equation 9, is similar to the reaction proposed by Choi *et al.* [5]. The approximate temperature dependence of the reaction is shown in Equation 10 where the error is estimated to be ±350 kJ. Equation 10 only incorporates the temperature dependence which arises from the reduction of sapphire, since the temperature dependence of the other reactions was not known. The details of the calculation are given in [17].

4.3. Growth kinetics of sputtered titanium films

A plot of the square of the Ti_3Al layer thickness divided by time versus $1/T$ is shown in Fig. 13. Fig. 13 is a plot of the general Equations 3 and 4. In thin film [8] and bulk reactions [11] between Ti and sapphire n has been found to equal 2, indicating diffusion-controlled growth. The layer growth observed in this study can be described by

$$(Ti_3Al\text{ layer thickness, nm})^2 = (3 \times 10^6) \times \exp(-24700/RT) \times (\text{time, sec}) \tag{11}$$

The plots shown in Fig. 13 result in almost identical activation energies. This agreement between the two different techniques indicates that the error in thickness measurement was not severe.

The significance of the activation energy, Q, depends on the system being studied. Kidson [10] derived equations describing the growth of intermediate layers in binary diffusion couples. For a three-phase system, a diffusion couple where an intermediate phase 'b' forms at the interface between the two end members 'a' and 'c' of the couple, the thickness of the intermediate phase 'b' is given by

$$W_b = \xi_{bc} - \xi_{ab} \tag{12}$$

where

$$\xi_{ab} = 2\left(\frac{(DK)_{ba} - (DK)_{ab}}{C_{ab} - C_{ba}}\right)t^{\frac{1}{2}},$$

$$\xi_{bc} = 2\left(\frac{(DK)_{cb} - (DK)_{bc}}{C_{bc} - C_{cb}}\right)t^{\frac{1}{2}}, \tag{13}$$

$$K = \left(\frac{\mathrm{d}c}{\mathrm{d}x}\right)_{ij}, \tag{14}$$

$$W_b = B_b t^{\frac{1}{2}} \tag{15}$$

The positions of the interfaces between the 'a' and 'b' phases and the 'b' and 'c' phases are represented by ξ_{ab} and ξ_{bc}, respectively. The concentration gradient, K, and the diffusivity, D, are evaluated in phase i at the ij interface. The slope of an Arrhenius plot of the thickness of the 'b' phase (Equation 12) does not give a simple activation energy. The slope obtained depends

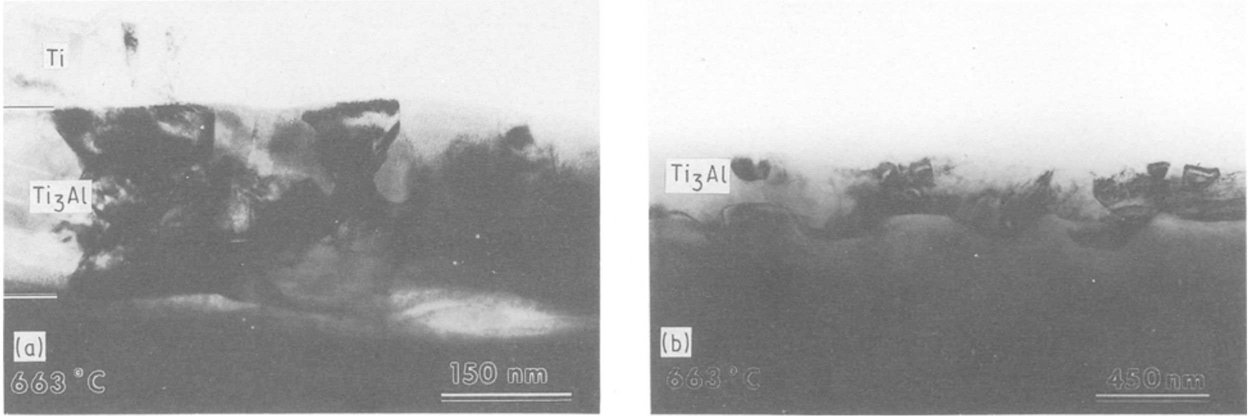

Figure 10 (a) TEM images of samples deposited and annealed for 2 hours at 663 °C, (b) shows signs of interface breakdown.

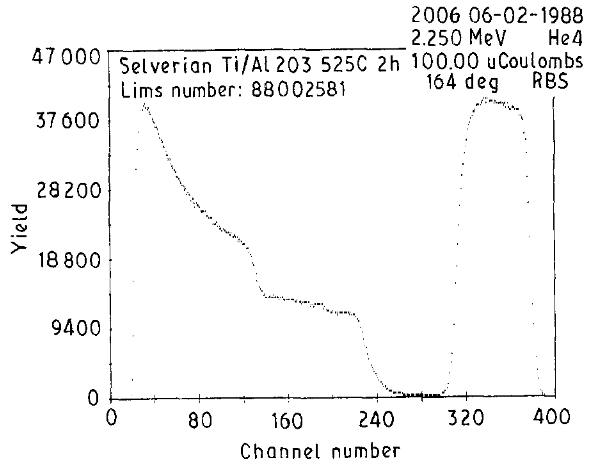

Figure 11 RBS spectrum from the sample deposited and annealed at 525 °C.

TABLE II Results of X-ray diffraction studies; (e) = evaporated Ti films and (s) = sputtered films

Heat treatment temperature, °C	Preferred orientation	
	Ti	Ti_3Al
25 (e)	(0 0 2)	not present
25 (s)	(0 0 2)	not present
525 (s)	(0 0 2)	(2 0 0)
554 (s)	random	(1 0 1)
562 (s)	(0 0 2)	random
580 (s)	(0 0 2)	(2 0 0)
630 (s)	(0 0 2)	(1 1 0)
663 (s)	(0 0 2)	(1 1 0)
825 (s)	not present	(1 1 0) or (0 0 2)

on the difference between the activation energies of the diffusivities in the '*a*', '*b*', and '*c*' phases. Consequently, the slope of the Arrhenius plot will not necessarily be a straight line, but may be curved. However, if an approximately straight line is obtained, it indicates that either: one of the diffusivities predominates; or that the diffusivities are similar to one another.

Kidson stated that there is nothing preventing the value of B_b in Equation 15 from becoming negative. A negative value of B_b indicates that the flow rate of material from the adjacent phase is so rapid that material cannot move through the '*b*' phase and material piles up in the '*b*' phase. When this occurs the

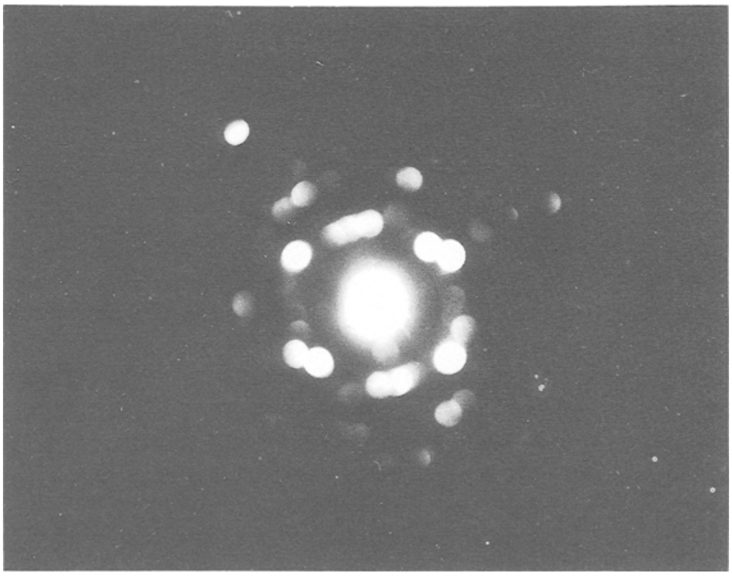

Figure 12 CBED pattern from the Ti film in the sample deposited at 25 °C, indicating no crystallographic alignment between the sputtered Ti and sapphire. No heat treatment.

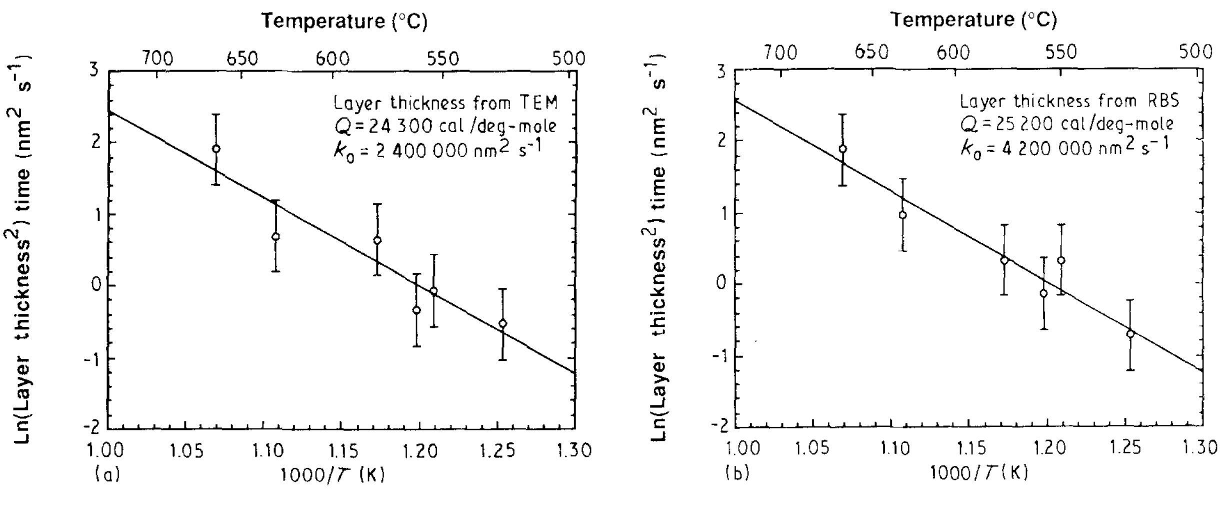

Figure 13 Arrhenius plots of Ti_3Al layer thickness after a 2 hour anneal: (a) layer thickness determined by TEM/AEM, (b) layer thickness determined by RBS.

next intermediate phase '*d*' would form and '*b*' would not grow or form.

Fig. 14 is an Arrhenius plot of D in Ti, Ti_3Al, and the quantity in Equation 16. The diffusivities in the Ti and Ti_3Al were approximated from the data of Hirano and Iijima [18] (Equations 17 and 18 below). The diffusivity for Ti in sapphire was approximated by the diffusivity of oxygen in sapphire [19] (Equation 19).

$$\left(\frac{(DK)_{cb} - (DK)_{bc}}{C_{bc} - C_{cb}}\right) - \left(\frac{(DK)_{ba} - (DK)_{ab}}{C_{ab} - C_{ba}}\right) \qquad (16)$$

$$D_{Ti} = 1.3 \times 10^{-8}\exp(-17\,800/RT)\ \text{cm}^2/\text{s} \qquad (17)$$

$$D_{Ti_3Al} = 3.66 \times 10^{-6}\exp(-29\,640/RT)\ \text{cm}^2/\text{s} \qquad (18)$$

$$D_{Al_2O_3} = 270\exp(-147\,000/RT)\ \text{cm}^2/\text{s} \qquad (19)$$

The diffusivity of Ti in sapphire is probably slower than the diffusivity of oxygen in sapphire. However, the diffusivity of oxygen in sapphire is so low that it did not influence the curve generated with Equation 16.

The values used in Equation 16 to calculate Fig. 14 are listed in Table III. The K_{ij} values in Table III were obtained by averaging values measured from the AEM traces. The slope of the straight line portion of the B_b curve is approximately 125 kJ/deg-mole.

The B_b line is curved over a small temperature range near 600 °C. Near 545 °C the value of B_b becomes negative, indicating that at temperatures below 545 °C the Ti_3Al phase should not appear. However, we have seen Ti_3Al at temperatures as low as 525 °C. This discrepancy can be explained by the fact that the values for C_{ij} and K_{ij} in Equation 16 were only approximate. Furthermore, Fig. 14 is only a rough approximation to the system presently studied since the current system is a ternary (Ti–Al–O). It is interesting, however, that in Fig. 8b there is a region where the Ti_3Al phase was not continuous. In the light of the discussion above, the existence of this non-continuous layer might be due to a change in the diffusivities resulting in B_b becoming negative.

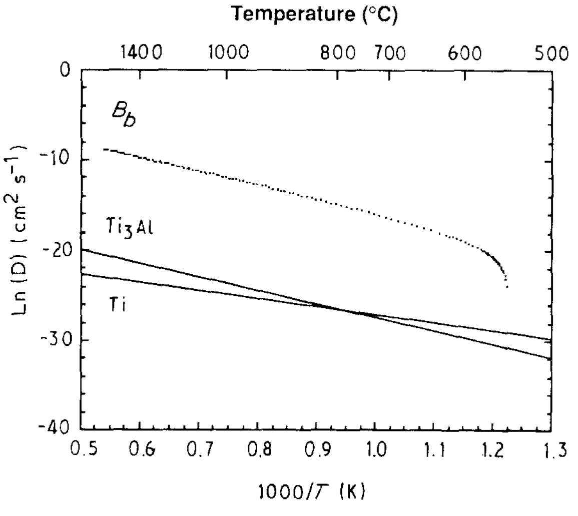

Figure 14 Plot of titanium and Ti_3Al diffusivities and B_b versus $1/T$.

TABLE III Values used in Equation 24

$(C_{bc} - C_{cb})$ (at. pct. Ti/nm)	$(C_{ab} - C_{ba})$	K_{cb}	K_{bc} (Ti atoms/cm^2)	K_{ab}	K_{ba}
−0.25	−0.75	3×10^3	9×10^3	2×10^5	2×10^4

From the discussions above the measured activation energy for the growth of the $Ti_3Al[O]$ layer, 103.4 ± 25 kJ/deg-mole in Equation 11, represents the activation energy for the growth of the Ti_3Al layer. However, it is not the activation energy of any specific process, but represents the activation energy of B_b.

4.3.1. *Effect of grain boundary on the growth of the Ti_3Al layer*

The grain size of a material has a large effect on the measured activation energy of diffusion. Grain boundary diffusion is expected to play a large role in diffusion processes at temperatures below one-half the melting point of the material.

The activation energy for bulk diffusion can be approximated by an empirical correlation between the melting temperature, T_m, and a constant of 150.7 J/K [20]

$$\frac{Q}{T_m} \approx 150.7\ \text{J/K} \qquad (20)$$

T_m is approximately 1900 K for titanium and Ti_3Al. Therefore, Q is expected to be approximately 293 kJ/deg-mole.

The present study and the two kinetic studies previously mentioned [8, 11] all show evidence that grain boundary diffusion played a significant role since activation energies much lower than 293 kJ/deg-mole were reported. Each study used different methods to prepare samples, resulting in different grain sizes and therefore varying amounts of grain boundary diffusion. The greater the contribution of grain boundary diffusion the lower the measured activation energy.

If grain boundary diffusion played a smaller role in the diffusion process, i.e., the material had a larger grain size, the activation energy and diffusivity would be smaller and the thickness of the Ti_3Al layer would also be smaller. This would be reflected in a higher activation energy for growth of the Ti_3Al.

5. Conclusions

The XPS study provided a fairly complete picture of the initial stages of the reaction between Ti and sapphire in the temperature range of 25 °C to 1250 °C. Titanium was seen to reduce sapphire at all temperatures studied to produce Ti–O bonds and Al involved in a metallic bond, probably with Ti, i.e. Ti–Al. Aluminum was seen in an intermediate oxidation state between 3+ and 0. This Al was probably due to mixed bonding across the interface. After a 2 hour anneal at 1250 °C, Ti was in the 2+ and 0 oxidation states and no evidence was seen for $Ti4^+$ or Ti^{3+}. The absence of the 3+ oxidation state indicates that

Ti does not substitute for Al in the sapphire lattice, within the sensitivity of XPS.

A possible structural and chemical picture of the Ti interface can be summarized as consisting of Ti–O bonds across an interface that is probably not wider than two atomic spacings. Ti–O bonds bridge the interface and the near-surface oxygen atoms in the sapphire form the majority of the chemical bonds with Ti while a small percentage of the interface bonding consists of mixed bonding between Ti, Al, and O.

Titanium films that were evaporated and sputter deposited from 25 °C to 825 °C on sapphire substrates all exhibited a strong (0 0 2) texture. However, the disordered $Ti_3Al[O]$ layers that grew upon annealing did not exhibit any strong texture. Although the Ti films did show a (0 0 2) texture, electron diffraction of several Ti grains revealed that the other degrees of freedom necessary for lattice matching between Ti and sapphire did not exist.

Titanium reduced sapphire to produce $Ti_{0.67}[O_{0.33}]$ and $Ti_3Al[O]$ according to

$$8Ti + Al_2O_3 = 3Ti_{0.67}[O_{0.33}] + 2Ti_3Al[O]$$

This reaction agrees well with that of Choi *et al.* [4] and of Chamberlain [8]. The reaction between Ti and sapphire is thermodynamically favourably at all temperatures studied.

The layer thickness measured by TEM/AEM and RBS was in agreement within the estimated errors associated with each technique. An activation energy of 103.4 ± 25 kJ/deg-mole for the growth of the $Ti_3Al[O]$ layer indicated that diffusion through the $Ti_3Al[O]$ grain boundaries was a significant contribution to the total diffusion process.

Acknowledgements

The authors would like to thank Dave Sokola and Albert Filo for their assistance.

References

1. K. R. KINSMAN, in "Electronic packaging and corrosion in microelectronics" (American Society for Metals, Ohio, 1987) p. 1.
2. D. HULL, in "An introduction to composite materials" (Cambridge University Press, 1981).
3. Y. S. CHAUG, N. J. CHOU and H. KIM, *J. Vac. Sci. Technol. A* **5(4)** (1987) 1288.
4. X. A. ZHAO, E. KOLAWA and M. A. NICOLET, *ibid.* **4(6)** (1986) 3139.
5. S. K. CHOI, L. FROYEN and M. J. BRABERS, in "High tech ceramics" (Elsevier Science Pub., Amsterdam, 1987) p. 407.
6. H. LEFAKIS, M. LIEHR, G. W. RUBLOFF and P.S. HO, in Materials Research Society Symposium Proceedings **Vol. 54** (Materials Research Society, Pittsburgh, 1986) p. 133.
7. C. P. LOFTON and W. E. SWARTZ, *Thin Solid Films* **52** (1978) 271.
8. M. B. CHAMBERLAIN, *J. Vac. Sci. Technol.* **15(2)** (1978) 240.
9. F. J. J. VAN LOO and G. D. RIECK, *Acta Metall.* **21** (1973) 73.
10. G. V. KIDSON, *J. Nucl. Mater.* **3(1)** (1961) 21.
11. R. E. TRESSLER and T. L. MOORE, *Met. Engng Q.* **February** (1971) 16.
12. W. CHU, J. M. MAYER and M. A. NICOLET, in "Backscattering spectrometry" (Academic Press, New York, 1978).
13. D. B. WILLIAMS, in "Practical analytical electron microscopy in materials science" (Philips Electronic Instruments Inc, Electron Optics Publishing Group, Mahwah, NJ, 1984).
14. G. ROCKER and W. GOPEL, *Sur. Sci.* **181** (1971) 530.
15. J. S. KIRKALDY and D. J. YOUNG, in "Diffusion in the condensed state" (The Institute of Metals, London, 1987) Ch. 11.
16. J. H. SELVERIAN, M. BORTZ, F. S. OHUCHI and M. R. NOTIS, in Materials Research Society Symposium Proceedings, Vol. 108 (Materials Research Society, Pittsburgh, 1988) p. 107.
17. J. H. SELVERIAN, in "Interface reactions and adhesion between titanium thin films and (0 1 2) sapphire substrates" Ph.D. dissertation (Lehigh University, Bethlehem, PA, 1988).
18. K. HIRANO and Y. IIJIMA, in "Diffusion in solids: recent developments" (The Metallurgical Society, Warrendale, 1984) p. 141.
19. K. P. R. REDDY and A. R. COOPER, *J. Amer. Ceram. Soc.* **65(12)** (1982) 634.
20. R. J. BORG and G. J. DIENES, in "An Introduction to solid state diffusion" (Academic Press Inc., New York, 1988) p. 61.
21. O. KUBASCHEWSKI and C. B. ALCOCK, in "Metallurgical thermochemistry" (Pergamon Press, New York, 1979).

Received 12 March
and accepted 2 August 1990